Combinatorial/High Throughput Methods for the Determination of Polyanhydride Phase Behavior

Jon B. Thorstenson, Latrisha K. Petersen, and Balaji Narasimhan*

Department of Chemical and Biological Engineering, Iowa State University, 2035 Sweeney Hall, Ames, Iowa 50011-2230

Received March 6, 2009

Combinatorial methods have been developed to study the phase behavior of biodegradable polyanhydrides for drug delivery applications. The polyanhydrides of interest are poly[1,6-bis(*p*-carboxyphenoxy) hexane] (CPH) and poly[sebacic anhydride] (SA). Both continuous and discrete polymer blend libraries were fabricated by using a combination of solution-based gradient deposition and rapid prototyping. Blend compositions were characterized via a high throughput transmission Fourier transform infrared (FTIR) sampling technique and compared against theoretical mass balance predictions. To obtain phase diagrams of CPH/SA, the effect of blend composition and annealing temperature on the miscibility of the blend was studied. This gradient library was observed with optical microscopy in order to determine cloud points. These results were compared with a theoretical phase diagram obtained from Flory−Huggins theory and with atomic force microscopy (AFM) experiments on blend libraries and the agreement between the methods was very good. The high throughput method demonstrates that the CPH/SA system exhibits upper critical solution temperature behavior. These libraries are amenable to other high throughput applications in biomaterials science including cell viability, cell activation, and protein/biomaterial interactions.

Introduction

The design of multicomponent polymer systems has become increasingly common in drug delivery, due to the time and effort required to design new carrier materials. In this regard, biodegradable copolymers based on esters and anhydrides have been well studied as drug carriers.[1] For the rational design of drug delivery carriers based on polymers, an understanding of the polymer phase behavior is important to tailor drug stabilization and release profiles. Information from the blend phase behavior, such as the Flory−Huggins parameter and phase transitions, can be used to describe microphase separation in block or weakly segregated random copolymers.[2,3] This microstructure of the polymer may play an important role in the release kinetics of drugs from these polymers.[4]

The present study is focused on the miscibility of blends based on the biodegradable polyanhydride homopolymers composed of 1,6-bis(*p*-carboxyphenoxy)hexane (CPH) and sebacic acid (SA) (Figure 1). Devices made from these polymers exhibit surface erosion as opposed to the bulk eroding mechanism exhibited by polyesters.[5,6] The surface erosion of CPH/SA is due to the hydrophobic nature of the aliphatic and aromatic moieties of the SA and CPH monomers, respectively. Surface erodible polymers have drug release profiles governed by erosion kinetics rather than diffusion and swelling that is the trademark of bulk eroding systems.[4] Due to the fact that poly(CPH) has a slower degradation rate than that of poly(SA), a phase separated drug delivery device will erode and release its payload at differing rates depending on the spatial position on the surface.[7] The overall release kinetics in a phase separated system is governed by the relative rates of degradation, the partition coefficient of the drug between the phases, and the relative amounts and composition of each phase.[7,8] Thus, an intimate knowledge of phase behavior is required to predict and tailor drug release kinetics.

The characterization of blend miscibility can be a time-consuming process if carried out by the conventional "one sample at a time" approach. The application of combinatorial and high throughput methods to phase behavior experimentation facilitates rapid scanning of parameter space for properties of interest. The biggest challenge in the implementation of combinatorial methods is library fabrication and high throughput screening. In the present study, we retrofit previously described sample preparation and characterization tools[9−13] for the study of polyanhydride phase behavior. A modification of the solution based flow-coating method developed by Meredith et al.[12] was used to create continuous

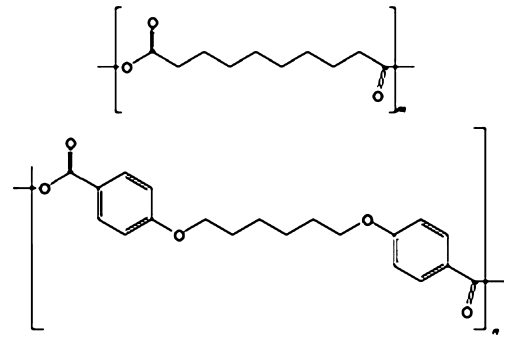

Figure 1. Structures of poly(SA) and poly(CPH).

* To whom correspondence should be addressed.

10.1021/cc900039k CCC: $40.75
Published on Web 08/19/2009

Table 1. Molecular Weight and Thermal Properties of Poly(CPH) and Poly(SA)

polymer	M_n (Da)	PDI	T_g (°C)	T_m (°C)
poly(CPH)	20438	2.04	46	143
poly(SA)	6889	2.43	62	82

gradient thin film libraries. A discrete methodology was adapted from the work of Cabral and Vogel in which thiolene arrays were imprinted on substrates using photolithography.[10,13] Both the continuous and discrete libraries were annealed on a temperature gradient stage and observed for the presence of cloud points. Flory−Huggins theory and previous work done by Kipper et al.[14] on the miscibility of CPH/SA blends were utilized in the theoretical determination of the phase boundary. Both the experimental and modeled phase diagrams were validated by conventional experiments.

Experimental Section

Materials. Norland optical adhesive 81 (NOA 81) was purchased from Norland Products, Inc. (Cranbury, NJ). Silicone based vacuum greases, NyeTorr 5300 and Nye Fluorocarbon Gel 811-1, were purchased from Tai Lubricants (New Castle, DE). IR transparent calcium fluoride wafers were obtained from Wilmad Labglass (Buena, NJ). Deuterated chloroform was purchased from Cambridge Isotope Laboratories (Andover, MA). HPLC-grade chloroform, acetic anhydride, methylene chloride, hexane, sulfuric acid, and acetic acid were purchased from Fischer Scientific (Hampton, NH). The chemicals 4-hydroxybenzoic acid, sebacic acid, and *N*-methyl-2-pyrolidinone were purchased from Sigma Aldrich (St. Louis, MO). 1,6-Dibromohexane was purchased from Acros (Fairlawn, NJ).

Polymer Synthesis and Characterization. Homopolymers of sebacic acid (SA) and 1,6-bis(*p*-carboxyphenoxy)-hexane (CPH) were prepared by the methods described elsewhere.[3,15−17] Prepolymer and monomer functionality was verified by proton nuclear magnetic resonance (^{1}H NMR) conducted on a Varian VXR 300 MHz spectrometer (Varian Inc., Palo Alto, CA). The chemical shifts exhibited by the samples dissolved in deuterated chloroform were calibrated with respect to the chloroform peak at $\delta = 7.26$ ppm. Number average molecular weights and polydispersity indices were determined by gel permeation chromatography (GPC). Samples were dissolved in HPLC-grade chloroform and separated on a Waters GPC chromatograph (Milford, MA) containing PL Gel columns (Polymer Laboratories, Amherst, MA). Elution times were compared to monodisperse polystyrene standards (Fluka, Milwaukee, WI). Polymer melting points and glass transition temperatures were determined by differential scanning calorimetry (DSC) thermograms obtained from a Q20 DSC (TA Instruments, New Castle, DE). Polymer samples were sealed in an aluminum DSC pan and heated from 25 to 180 °C and then quenched back down to room temperature at a rate of 10 °C/min. Representative properties for poly(SA) and poly-(CPH) are shown in Table 1.

Continuous Library Fabrication. Continuous combinatorial polyanhydride libraries were fabricated by modifying a method described by Meredith et al.[12] The preparation of these libraries can be divided into three steps: gradient mixing, gradient deposition, and film spreading. In gradient mixing, one push−pull syringe pump (KDS120, KD Scientific, MA) was used to infuse a poly(CPH) solution (2 wt % in chloroform) into a 20 mL scintillation mixing vial ($V =$ 8 mL of 2 wt % SA in chloroform) while simultaneously maintaining the vial volume by way of the withdraw side of the pump. Both syringes on the mixing pump were operated at a volumetric flow rate (I and W, respectively) of 60 mL/h. The syringe pair on the push−pull pump consisted of two 10 mL syringes (Popper, Hyde Park, NY) connected to 24 in. long, 20 gauge stainless steel capillaries. As this dynamic mixing process was taking place, a second syringe pump (NE-1000, New Era, Farmingdale, NY) with a 500 μL syringe (Hamilton, Reno, NV) was used to withdraw a sample of the time dependent concentration fluctuation. A three part 13 μL sample was drawn up at a rate of $S = 42$ μL/h into a 20 gauge stainless steel capillary tube. The first 3 μL were withdrawn 2 s before the mixing process began, the next 7 μL represented the desired concentration gradient, and the last 3 μL was taken after the mixing process had completed. The presence of the buffer solutions and the dimensions of the gradient have important implications for gradient deposition.

In gradient deposition, a robotic sample manipulator was utilized to deposit the gradient contained in the capillary tube into the form of a line on a 50 mm × 3 mm calcium fluoride wafer (Thermo Scientific, Waltham, MA). The robotic apparatus was comprised of a custom-made sample holder situated on a 60 mm translation stage (TSB60-I, Zaber, Richmond British Columbia, Canada) with a 60 mm linear actuator (KT-LA60A, Zaber). A notable feature of the custom fabricated sample holder is the presence of cooling coils wrapped around the base. The coils, together with a circulating bath, glovebox, and dehumidifier, can be used to inhibit solvent evaporation between gradient deposition and film spreading.

Once the gradient mixing process was completed, the capillary containing the three-part sample was positioned over the sample-manipulating robot in such a way that the tip of the capillary was 7.5 mm from the edge of the CaF_2 wafer. The deposition of the sample was done at a volumetric flow rate of 2518 μL/h and was started in conjunction with the movement of the wafer underneath the capillary tip such that the wafer velocity matched the fluid dispensing velocity. In this way, the length of the gradient deposited onto the substrate matches the length of the gradient in the capillary. The absence of gradient compression during deposition ensures that detrimental mixing does not occur.

The first 3 μL buffer section was dispensed from the capillary while the deposition robot moved the 7.5 mm distance between the tip and the substrate. The buffer was not deposited on the substrate but was wiped from the capillary tip just as it contacted the edge of the wafer. The purpose of this initial buffer was to spare the gradient of any deleterious evaporation in the time required to accurately position the sample capillary tip prior to deposition. At the moment the tip reached the edge of the substrate, the desired gradient started to deposit. Once the 7 μL sample was

dispensed, the syringe pump stopped so that the last buffer section remained in the capillary. The purpose of this buffer section was to account for lag in the syringe pump stepper motor at the initiation of sample withdrawal from the mixing vial during gradient mixing.

Film spreading was used to spread the deposited line orthogonal to its gradient so that a two-dimensional thin film is formed. The process of spreading the film was accomplished by means of a second robotic apparatus consisting of a glass knife-edge attached to a linear stepper motor. The base of the apparatus, which provided accurate placement of the knife-edge, was formed by a 90° bracket (model 360-90, Newport, Irvine, CA) attached to an *XZ* axis positioning stage (model 462-XZ, Newport). On top of this mounting platform were a 60 mm linear stage (TSB60-I, Zaber) and actuator (KT-LA60A, Zaber), tilt platform (model 36, Newport), and custom-made knife-edge armature. The tilt platform provided a 5° angle between the glass knife-edge and calcium fluoride wafer. The spreading of the gradient by the stepper motor was done at a velocity of 4 mm/s after which most of the solvent had evaporated. Any residual solvent was removed during an annealing step prior to characterization using optical microscopy.

A quantitative prediction of the gradient composition in terms of poly(SA) mass fraction as a function of time (minutes) can be derived[12] and is represented by eqs 1 and 2.

$$x_{SA,(vial)} = x_{SA,0}\left[\frac{1 - ((I - W - S)t + M_0)}{M_0}\right]^{(-I/(I-W-S))} \quad (1)$$

$$\phi_{SA,(film)} = \frac{x_{SA,(vial)}}{(x_{SA,(vial)} + x_{CPH,(vial)})} \quad (2)$$

Here, I = infusion rate (mL/min), W = withdrawal rate (mL/min), S = sampling rate (mL/min), M_0 = initial vial volume (mL), t = time (min), $x_{SA,0}$ = initial mass fraction of SA, and ϕ_{SA} = mass fraction of SA in the film.

The material balance (eq 1) denotes the mass fraction of poly(SA) in the vial as a function of initial poly(SA) concentration in the vial, initial vial volume, time, and the volumetric flow rate of the infuse, withdraw, and sample pumps. The mass fraction of poly(SA) after deposition (eq 2) represents the ratio of the poly(SA) mass fraction in the film and the sum of the poly(SA) and poly(CPH) mass fractions in the mixing vial. As discussed later, these equations are useful both for experimental design and for validation of the high throughput characterization results.

Discrete Library Fabrication. Thiolene Well Plate Fabrication. The fabrication of discrete well plates was accomplished by a modified photolithography method previously described by various authors.[9,11,13,18] The basic idea is to form wall-like structures by selectively polymerizing areas of a thiolene-based resin by means of a collimated UV source and discriminating mask. The UV mask was designed using MS Word and printed out on a standard black and white laser printer. These templates were then converted into transparencies and layered on top of one another to obtain a mask that exhibits both high resolution and contrast. Black electrical tape was used to affix four mask layers to a standard

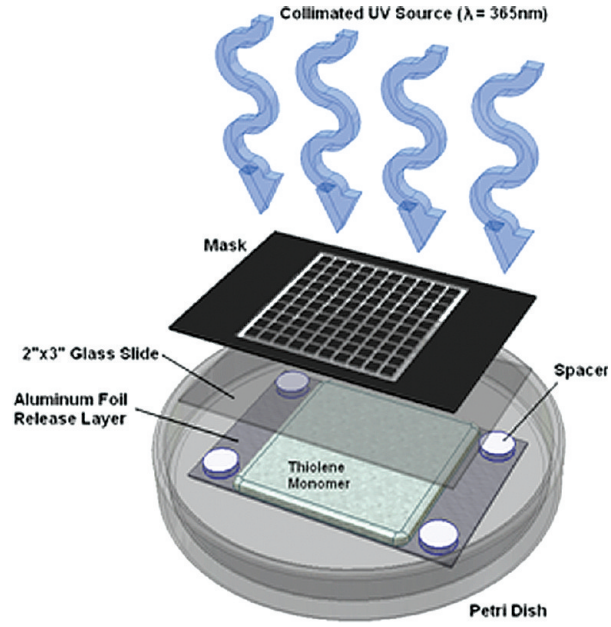

Figure 2. Schematic of photolithographic design of discrete thiolene well substrates.

2 in. × 3 in. borosilicate glass slide, which provided both mechanical integrity and a flat surface with which to polymerize on. Stainless steel spacers were then positioned and adhered to the outside corners of the glass slide to form an upper limit on the thickness of the polymerizing resin. A release layer of aluminum foil was used instead of polydimethylsiloxane (PDMS Sylgard 184 Base and PDMS Sylgard 184 Cure (Dow Corning, Midland, MI)) employed by other researchers.[9,11,13,18] PDMS films require a cure time of 12 h and often result in uneven features, which have a detrimental effect on the uniformity of the resulting thiolene device.

As shown in Figure 2, a standard 4 in. i.d. plastic Petri dish was used as a platform for the overall photolithography process. Once the aluminum foil release layer was placed in the Petri dish, a small amount of NOA 81 (~5−10 mL) was poured over the top. The mask−substrate assembly was carefully positioned over the unreacted thiolene in such a way as to avoid the trapping of air bubbles. The whole setup was exposed to a collimated UV lamp (λ = 365 nm) at an intensity of 25 mW/cm^2. After 5 min, the aluminum foil release layer was carefully peeled away to expose the partially cured thiolene and unreacted monomer.

As opposed to removing unreacted thiolene from the multiwell device with ethanol or acetone, the thiolene array itself was stripped from the glass substrate and subjected to gentle bursts of compressed air to remove the bulk of the monomer. A residual amount of unreacted thiolene was left on the bottom of the array so that it could be adhered to another substrate. The benefit of total array delamination before postcuring is that perfectly clean well bottoms can be achieved and substrates other than glass can be utilized. Cured arrays for cloud point observation (10 wells × 10 wells) were reattached to 2 in. × 3 in. glass slides. For high throughput Fourier transform infrared (FTIR) quantification, 5 × 4 arrays (discussed below) were bonded to double polished 2 in. i.d. silicon wafers (University Wafer, South

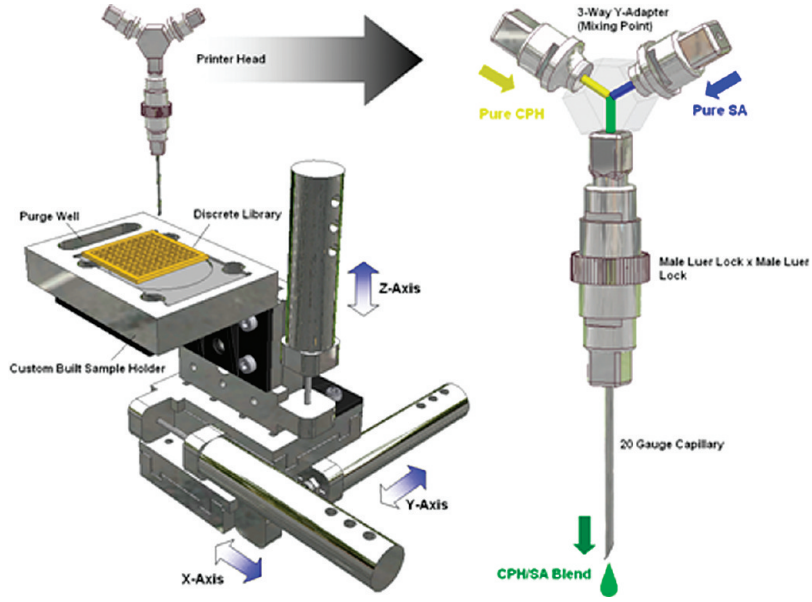

Figure 3. Schematic of microfluidic dispensing apparatus.

Boston, MA). Each of the two array types was postcured under UV light for 30 min at 50 mW/cm^2. Finally, the discrete well substrates were thermally cured for 5 h at 180 °C.

Microfluidic Dispensing Apparatus. Libraries of linearly varying composition of CPH/SA were fabricated at high throughput using microfluidics and robotics. The deposition of homopolymer solutions (1.5 wt % in HPLC grade chloroform) was achieved by using two programmable syringe pumps (New Era Pump Systems) each equipped with a 10 mL luer lock glass syringe (Popper) connected to a 24 in. long, 20 gauge stainless steel capillary tube. In order to produce homogenized droplets of sufficiently low volume (~15 μL), it was necessary to bring the CPH and SA source pumps together at a mixing point prior to droplet formation. The printer head, shown in Figure 3, was comprised of a 3 way Y-adapter (C-31507-81, Cole-Parmer, Vernon Hills, IL) connected to a male−male luer lock adapter (C-31507-55, Cole-Parmer) and a 12 in. long, 20 gauge luer lock capillary. To produce a desired composition, the syringe pumps first purged the printer head of the previous mix ratio. For example, if a 25/75 CPH/SA vol % droplet was required, the SA syringe pump would have a flow rate three times that of the CPH pump. Started simultaneously, the dual pumps had a combined flow rate of 0.5 mL/min and total running time of 120 s. The 2 mL CPH/SA solution delivered by the pumps during the purge operation was more than enough to reset the printer head for the next deposition. Once the printer head was flushed of the previous sample, droplets could be dispensed into discrete well substrates for a total volume not to exceed 200 μL. This threshold represents the maximum allowable sample volume without contamination by the single pump pushing the droplets through the printer head. The upper limit on the available sample can be increased by lengthening the printer tip capillary.

The *XYZ* translational positioning of discrete substrates underneath the stationary printer head was accomplished by means of three programmable, motorized stages arranged orthogonally. The *X*−*Y* translation plane was controlled by two 60 mm linear stages (TSB60-IV, Zaber, Richmond, British Columbia, Canada) powered by two stepper motor actuators (KT-LA60A-SV, Zaber). The *Z*-axis was comprised of a single 28 mm linear stage (TSB28-IV, Zaber) and actuator (KT-LA28A-SV, Zaber). Angle brackets (AB90-I, Zaber) were used to connect the *Z*-axis with the *X*−*Y* stages and a custom-built sample holder. A well was milled into the sample holder to act as a reservoir for the purge operation of the printer head. To reduce friction and sticktion in the drive screws, NyeTorr 5300 lubricant (Tai Lubricants, New Castle, DE) was sparingly applied to the drive threads. Integration and control of the syringe pumps and positioning robot was achieved with the use of third-party macro software (Insight Software Solutions, Kaysville, UT) alternately communicating with the pumps (DOS) and stages (Visual Basic) via RS232 communication lines.

For phase boundary observation, a 10 × 10 well plate format was adopted in which each column in the array contained a uniform composition ranging from 10/90 to 60/40 vol % CPH/SA across the ten rows. Characterization by FTIR microspectroscopy was carried out by pooling together each column in the phase behavior library and depositing them as a whole into a 5 × 4 array (repeated twice per substrate). The more open features of the 5 × 4 device (7.4 mm × 7.4 mm × 3 mm) made it possible to conduct transmission mode FTIR while avoiding interference due to the thiolene.

High Throughput Library Characterization—FTIR. The composition gradient was characterized via high throughput transmission mode FTIR spectroscopy. The mole fraction of poly(CPH) as a function of position was determined by calculating the area ratio of a characteristic poly(CPH) peak to a characteristic poly(SA) peak and comparing that ratio to a previously prepared calibration curve. Once the characteristic peaks were chosen, a calibration curve was constructed by collecting FTIR spectra of polymer thin films ranging from blend compositions of 10:90 to 90:10 CPH:SA in increments of 10 mol %. Standards of blend solutions consisting of 1 wt % CPH/SA polymer in HPLC grade chloroform were spun cast onto infrared transmissive calcium

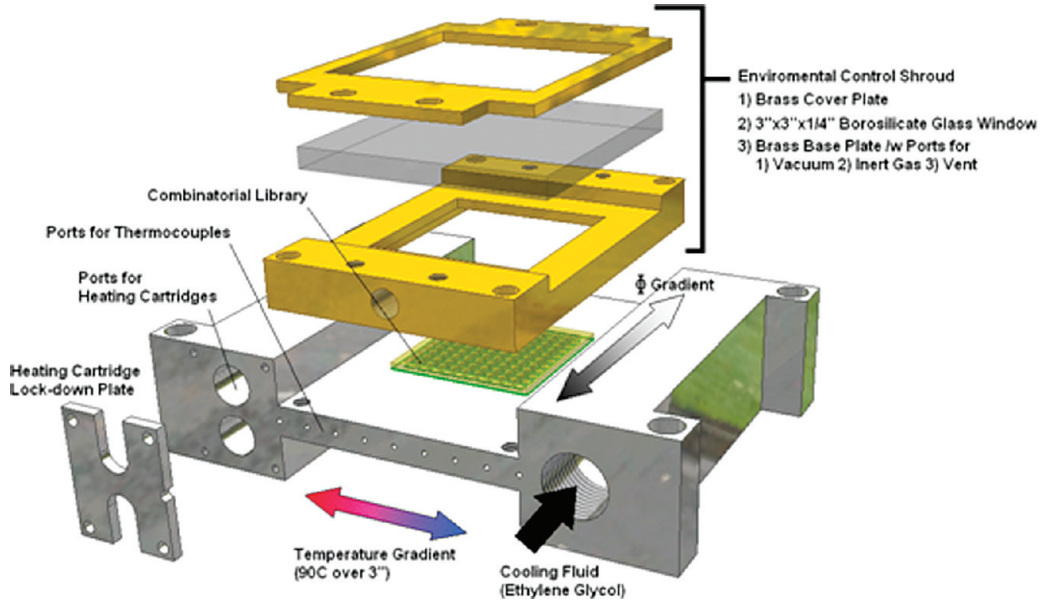

Figure 4. Schematic of linear temperature gradient stage.

fluoride wafers at 1500 rpm for 30 s using a spin coater (Headway Research Inc., Garland, TX). The thin film samples were dried at room temperature and pressure for 1 h. Spectral data of the calibration standards was obtained on a Nicolet 6700 FTIR spectrometer (Thermo Scientific). Line maps and discrete point maps were collected for continuous and discrete libraries respectively on a Nicolet Continuum infrared microscope (Thermo Scientific) outfitted with a liquid nitrogen cooled mercury cadmium telluride (MCT) detector and an $X-Y$ robotic translation stage. Two hundred scans were collected for each data point at a resolution of 4 cm^{-1} and nitrogen purge flow rate of 30 SCFH.

High Throughput Phase Behavior Characterization—Optical Microscopy. Both the continuous and discrete libraries were annealed on a custom-built, continuous temperature gradient stage and observed via optical microscopy for the existence of the polymer blend phase boundary. The continuous temperature gradient stage consisted of a (6 in. × 4.5 in. × 1.5 in.) block of aluminum heated on one side by a 470W heating cartridge (CSH-304470/120 V, Omega, Stamford, CT) and cooled on the other side by an ethylene glycol circulating bath (1162A, VWR, West Chester, PA). Pure ethylene glycol was utilized as a coolant for both its thermal stability (T_b = 197 °C) and its excellent fluidic characteristics (SG = 1.1). The 1/2 in. i.d., 4 in. long heating cartridge was controlled by a proportional, integral, derivative (PID) autotune temperature controller (CN9000A, Omega). An environmental control shroud made of brass was utilized to prevent sample oxidation and to expedite phase transitions via partial pressure reduction.[19] A 3 in. × 3 in. × 1/4 in. slab of borosilicate glass formed the viewing window, which was clamped down to the *T*-gradient stage and sealed with Viton gaskets (Scientific Instrument Services, Ringoes, NJ). Three 1/4 in. NPT ball valves were affixed to the shroud base allowing for vacuum, inert gas, and vent connections. Thermocouple ports for K-type penetration probes (SMP-NP-K-125G-6, Omega) were situated along the base of the heating block to assist in temperature profile determination. Figure 4 shows a schematic of the *T*-gradient stage and environmental control shroud. The accuracy of the *T*-gradient stage was measured to be ±2 °C.

Libraries were heated past the melting points of both polymers prior to annealing on the *T*-gradient stage in order to erase thermal history. To accomplish this, the cooling side of the temperature stage was shut down, allowing the heating cartridges to establish a uniform temperature. After 1 h the *T*-gradient was brought online by adjusting the heater set point and initiating the cooling bath. Once the library was exposed to the linear temperature gradient, it was allowed to equilibrate for several hours before the phase boundary was captured optically by a charge-coupled device (CCD) camera (KP-M2U, Hitachi Kokusai Electric Inc., Tokyo, Japan) equipped with an adjustable focus lens (AF Micro-Nikkor 60 mm f/2.8D, Nikon, Melville, NY).

Validation of High Throughput Phase Behavior—Atomic Force Microscopy (AFM). Poly(SA)/poly(CPH) blend libraries were created by spin-casting at 1500 rpm for 30 s on clean Si wafers (with gold coating) using a spin coater (Headway Research Inc., Garland, TX) from a 1% (w/v) solution of polymer in HPLC-grade chloroform, filtered through 0.2 mm PVDF membrane syringe filters (Pall Gelman, Portsmouth, UK), resulting in 200 nm films.[14] Films were dried at room temperature for 1 h and annealed at 25, 90, and 180 °C for up to 12 h under vacuum (10^{-3} Torr). Annealed films were quenched with liquid nitrogen to below the glass transition temperature, in order to "freeze" the phase morphology prior to AFM experiments. AFM images of surface topography were obtained on a Dimension 3000 scanning probe microscope (Digital Instruments, Santa Barbara, CA). The AFM was operated in contact mode using Ultrasharp silicon cantilevers (Mikromasch, Tallinn, Estonia) with a force constant of 0.30 N/m. Root-mean-square roughness was computed from AFM measurements.

Results and Discussion

FTIR—Calibration and Quantification. A typical IR spectrum of a poly(CPH)/poly(SA) blend is shown in

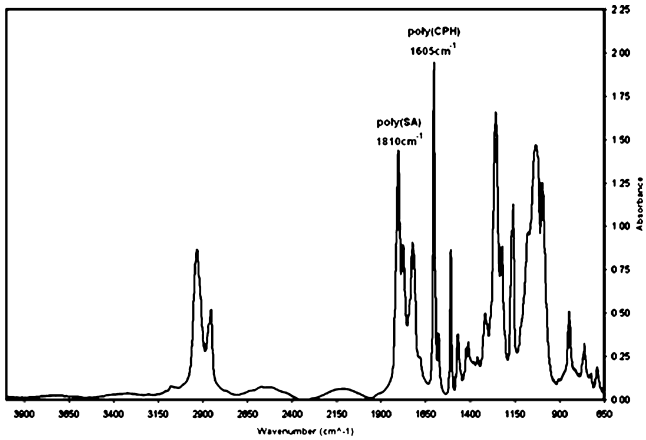

Figure 5. Representative FTIR spectrum of a 60/40 (mol %) poly(CPH)/poly(SA) blend.

Figure 5. The characteristic peak chosen for poly(CPH) is a sharply defined peak at 1605 cm^{-1} that represents aromatic ring stretching.[13] The feature chosen for poly(SA) is at 1810 cm^{-1} and represents the carboxyl antisymmetric stretching of the aliphatic-aliphatic anhydride bond.[13]

Since the IR data (Figure 5) is a spectral aggregate representing the summation of multiple smaller peaks in close proximity, a mathematical deconvolution of the raw data is necessary to ascertain the spectral contribution of a single band. The constituent peaks were modeled by a normal standard distribution (Gaussian function). Equations 3 and 4 were used to model the area occupied by overall spectra.

$$y(x) = \phi_1\left[\frac{1}{\sigma_1\sqrt{2\pi}}e^{-(x-\mu_1)^2/2\sigma_1^2}\right] + \phi_2\left[\frac{1}{\sigma_2\sqrt{2\pi}}e^{-(x-\mu_2)^2/2\sigma_2^2}\right] + \phi_3\left[\frac{1}{\sigma_3\sqrt{2\pi}}e^{-(x-\mu_3)^2/2\sigma_3^2}\right] + \phi_4\left[\frac{1}{\sigma_4\sqrt{2\pi}}e^{-(x-\mu_4)^2/2\sigma_4^2}\right] \quad (3)$$

$$\left[\sum_{x=400\text{cm}^{-1}}^{4000\text{cm}^{-1}} y_{\text{actual}}(x) - \sum_{x=400\text{cm}^{-1}}^{4000\text{cm}^{-1}} y_{\text{model}}(x)\right]^2 = 0 \quad (4)$$

Here, y = value of the distribution (absorption), x = the value for which the distribution is sought (wavenumber, $-\infty < x < \infty$), μ = arithmetic mean, σ = standard deviation ($\sigma > 0$), and φ = relative contribution of the distribution to spectrum as a whole (CPH: $\varphi_1 \rightarrow \varphi_4$, SA: $\varphi_1 \rightarrow \varphi_3$).[20]

The CPH/SA spectrum was divided into two regions (1650−1850 cm^{-1} for SA and 1495−1630 cm^{-1} for CPH) with each containing a characteristic peak.[13] In each experiment, the actual data collected from the spectrometer was modeled with Gaussian functions and the unknown variables for each peak (μ, σ) were determined iteratively using MS Excel Solver by employing eq 4 as the forcing function.

The calculated peak areas for CPH (1605 cm^{-1}) and SA (1810 cm^{-1}) were divided by one another and divided by their respective monomer molecular weights in order to account for the effect that differing values of M_r might have on the area of the characteristic peak. The peak areas were also divided by their respective number of occurrences of characteristic peak functionality per monomer. Since the characteristic functionality for CPH (aromatic ring) and SA (aliphatic−aliphatic anhydride bond) both occur twice per monomer unit, the effect on the following equation can be factored out.

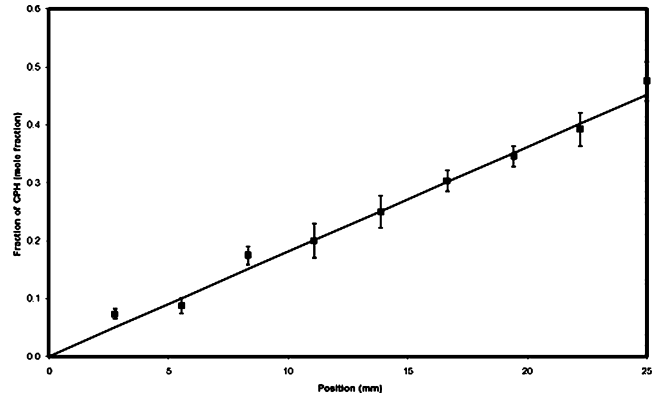

Figure 6. Experimentally measured composition profile in a poly(CPH)/poly(SA) blend continuous library. The line represents the mass balance as predicted by eqs 1 and 2.

$$X_{\text{CPH,measured}} = \frac{\dfrac{\text{area}_{\text{CPH,1605cm}^{-1}}}{2M_{\text{r,CPH}}}}{\dfrac{\text{area}_{\text{SA,1810cm}^{-1}}}{2M_{\text{r,SA}}} + \dfrac{\text{area}_{\text{CPH,1605cm}^{-1}}}{2M_{\text{r,CPH}}}} = \frac{\dfrac{\text{area}_{\text{CPH,1605cm}^{-1}}}{M_{\text{r,CPH}}}}{\dfrac{\text{area}_{\text{SA,1810cm}^{-1}}}{M_{\text{r,SA}}} + \dfrac{\text{area}_{\text{CPH,1605cm}^{-1}}}{M_{\text{r,CPH}}}} \quad (5)$$

Here, $X_{\text{CPH,measured}}$ = calculated CPH area ratio, $\text{area}_{\text{CPH,1605cm}^{-1}}$ = measured CPH characteristic peak area, $\text{area}_{\text{SA,1810cm}^{-1}}$ = measured SA characteristic peak area, $M_{\text{r,CPH}}$ = CPH monomer molecular weight (340 g/mol), and $M_{\text{r,SA}}$ = SA monomer molecular weight (184 g/mol). In order to obtain CPH mole fractions, the measured area ratios collected from standard solutions (described previously) were plotted against their known CPH content. The resulting data was fitted with a quadratic polynomial with an R^2 value of 0.9951. The trend line function was used in conjunction with the expression for the measured CPH ratio (eq 5) to yield an equation for actual CPH mole fraction.

FTIR−Continuous and Discrete Libraries. Characterization of polymer thin films via transmission, specular reflectance, and reflection−absorption FTIR modes has been utilized in many different combinatorial and high throughput applications. Specular reflectance of thick polymer films was used by Sormana et al.[21] to study the effect of chain extender composition on the mechanical properties of segmented poly(urethane−urea)s. The reflection−absorption technique has been utilized by Simon and Eidelman[22−24] to investigate the effect of poly(L-lactic acid)/poly(D,L-lactic acid) blend composition on cell proliferation and mechanical modulus. Transmission mode FTIR was employed by Martin et al.[25] to characterize poly(diethylaminoethylacrylate)/poly(dimethylaminomethylstyrene) thin films deposited on IR transmissive silicon wafers via combinatorially initiated chemical vapor deposition. Transmission mode was chosen to quantify the compositional gradients of both the continuous and discrete methodologies. The pairing of discrete well libraries

Table 2. Calculation of the Range of Possible Reynolds Numbers for the Gradient Sampling Syringe and Capillary

	diameter D (mm)	viscosity μ (kg/m·h)	density ρ (g/cm^3)	minimum velocity v (mm/s)	maximum velocity v (mm/s)	minimum *Re*	maximum *Re*
500 μL syringe	3.26	1.93	1.49	9.99×10^{-5}	0.212	0.001	1.9
20 gauge capillary	0.595	1.93	1.49	2.98×10^{-3}	6.35	0.005	10.5

with high throughput transmission FTIR has been explored in an attempt to design a characterization technique more reliable and easier to automate than other spectroscopic methodologies.[26]

Figure 6 shows the experimentally measured composition profile of a CPH/SA continuous library. A linear profile ranging from 10/90 to 60/40 CPH/SA vol % was measured in accordance with the mixing parameters (described earlier) prescribed by the mass balance (eqs 1 and 2). An upper threshold of 60/40 CPH/SA vol % was chosen due to the previous findings of Kipper et al.[14,27] The semicrystalline nature of poly(SA) and poly(CPH) has the potential to introduce inhomogeneities that can easily be mistaken for phase separation induced microstructure. The relatively low melting point of poly(SA) ($T_{M,SA} = 82$ °C) negates the ability of poly(SA) rich formulations to develop crystalline features near the critical point. Compositions rich in poly(CPH) on the other hand, do not experience loss of crystallinity until well above the phase boundary when the melting point of CPH is reached ($T_{M,CPH} = 143$ °C). Apparent cloud points for high poly(CPH) regions approach its melting point, thus indicating a difficulty in discerning crystallinity and phase microstructure.[14,27] This problem is further compounded by the fact that crystallinity and phase separation features are on the order of the resolution of optical microscopy (1 μm). These issues are partially alleviated with the use of ex situ AFM on blend libraries as described below.

The state of fluid flow in the sampling capillary and syringe were examined in order to ascertain the presence of any detrimental turbulent mixing conditions. Because the gradient solution was very dilute, the values of viscosity and density were assumed to be equal to that of pure chloroform. With this in mind, the ranges of possible values for the Reynolds number ($Re = Dv\rho/\mu$) were calculated for the minimum and maximum velocities for the syringe and capillary as set by the syringe pump capabilities. It can be observed from Table 2 that regardless of velocity chosen for gradient sample withdrawal or deposition, *Re* remains less than 10.5. Because the maximum *Re* was far below the turbulent transition ($Re \approx 2100-4000$), conservation of the gradient was ensured.

The composition gradient of a CPH/SA discrete library measured via the thiolene/silicon array methodology is shown in Figure 7. As with the continuous library, a composition range of 10/90 to 60/40 CPH/SA vol % was employed. The linearity of the profile spanning the library demonstrates not only the accuracy of the printer head mixing conditions but also the viability of the thiolene/silicon substrate as a platform for high throughput transmission FTIR characterization.

Optical Microscopy. Both the continuous and discrete libraries were annealed on the continuous temperature gradient stage and observed via optical microscopy for the existence of the polymer blend phase boundary. The phase boundary separating the miscible and immiscible regions of the library was visible due to differences in opacity. The miscible region appears translucent and turns opaque upon crossing the binodal into the immiscible region. The formation of microdomains during spinodal decomposition causes a change in the index of refraction, which in turn defines opacity. The temperature profile used to anneal the libraries orthogonal to their applied concentration gradient is shown in Figure 8.

Optical microscopy images of a discrete and continuous library annealed with a temperature gradient are shown in Figure 9. Libraries for microscopy were fabricated with minor differences from their FTIR counterparts. In order to improve visual contrast between the polymer and surrounding thiolene, the discrete library was printed into the same 10 × 10 array three times resulting in films with an estimated thickness of 30 μm. This estimation assumed a density of 1.1 g/cm^3 for both poly(SA) and poly(CPH).[14,27] Placing a silicon wafer underneath the annealing library also improved contrast. The continuous library was created with twice the polymer concentration (4 wt %) both to improve contrast

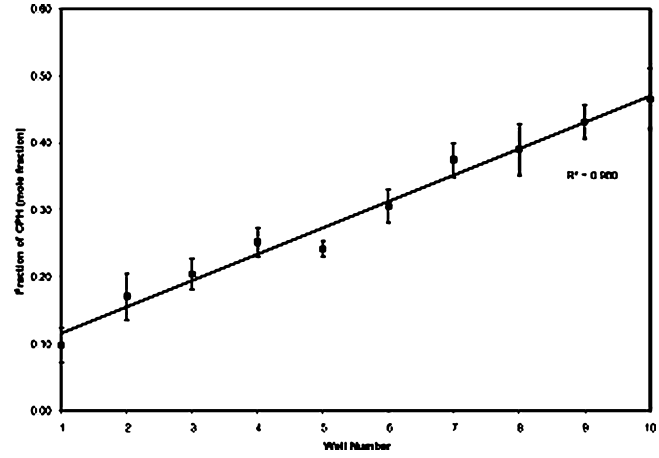

Figure 7. Experimentally measured composition profile in a poly(CPH)/poly(SA) blend discrete library. A trend line is shown to exemplify the linearity of the gradient across each well.

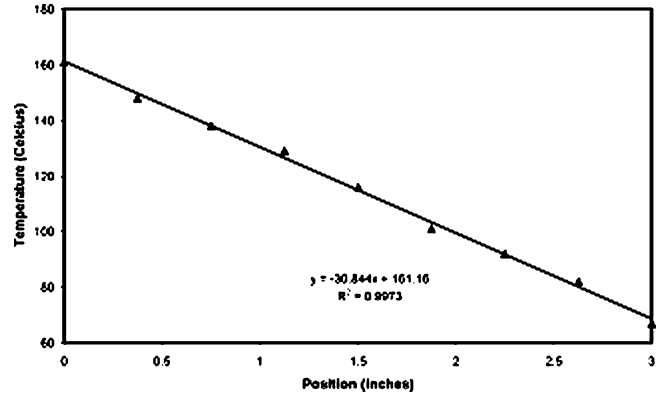

Figure 8. Experimental temperature profile for the *T*-gradient stage. A trend line is shown to exemplify the linearity of the gradient across the heating block.

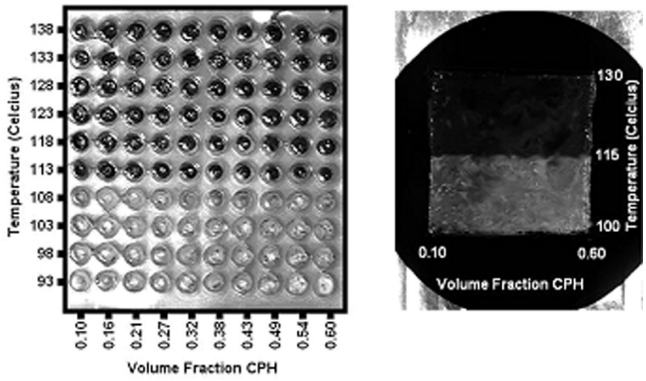

Figure 9. Discrete and continuous experimental phase diagrams for poly(CPH)/poly(SA) blends.

and to prevent dewetting. The resulting film was estimated to be around 800 nm thick. For improved thermal contact, the continuous films were spread on silicon wafers instead of calcium fluoride.

Both libraries exhibited a flat profile phase boundary (that occurs at 113 °C for the discrete library and at 115 °C for the continuous library). Both libraries show that the poly(CPH)/poly(SA) blend exhibits upper critical solution temperature (UCST) behavior and resulted in critical points there were in very good agreement with each other. This is also consistent with previous work that shows that the CPH/SA system exhibits UCST behavior.[14] The degrees of polymerization for the CPH/SA homopolymers ($N_{CPH} = 59$, $N_{SA} = 38$) result in a fairly symmetric phase boundary.

AFM. To complement and validate the optical microscopy experiments, ex situ AFM experiments were performed. The AFM experiments enabled the determination of the phase morphology, providing additional information on the phase behavior obtained from the cloud points observed in optical microscopy. Additionally, the higher resolution of AFM enabled the observation of phase behavior in the poly(CPH)-rich regions of the phase diagram and distinguish crystallization from amorphous phase separation. Further, these experiments validated the phase diagram obtained from the high throughput optical microscopy data. Figure 10A shows 5 μm × 5 μm scans of the 49/51 CPH/SA blend composition of the two polymers annealed at 25, 90, and 180 °C. The images show spherical droplets of one phase (i.e., SA) at 25 and 90 °C, indicative of phase separation at these annealing conditions. These morphologies are consistent with a phase-separated system as obtained by the high throughput optical microscopy data. When the blend was annealed at 180 °C, the film displayed a smooth and homogeneous surface, indicative of a one-phase system. This is also consistent with the phase diagram in Figure 9, which predicts a one-phase system above ~115 °C. Similar information was obtained for the other blend compositions studied (data not shown). The root-mean-square roughness obtained from AFM for the blend library as a function of annealing temperature and blend composition is shown in Figure 10B. The data indicates that the surface roughness for the phase-separated films is an order of magnitude higher than that for the homogeneous films. Additionally, in the phase-separated region (which is below the melting point of poly(CPH)), the rms roughness increases with increasing poly(CPH) content in the blend,

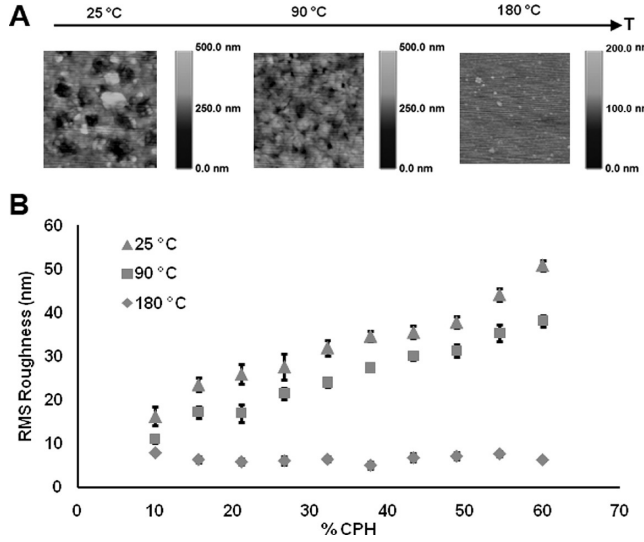

Figure 10. (A) 5 μm × 5 μm AFM scans of 49/51 poly(CPH)/poly(SA) blend annealed at three different temperatures (25, 90, and 180 °C). (B) Root-mean-square roughness of the blend surfaces as a function of blend composition and annealing temperature. Error bars represent standard deviation with $n = 6$.

as expected. In summary, the phase behavior observed in the AFM scans is consistent with the phase diagram shown in Figure 9.

Conclusions

Continuous and discrete library methodologies were designed for the combinatorial and high throughput determination of polyanhydride blend phase behavior. The continuous gradients were fabricated by using a three step solution-based flow coating method. Discrete gradient arrays were rapidly prototyped with an *XYZ* translational robot and microfluidic printer head. Blend compositional profiles were quantified by high throughput transmission FTIR. A thiolene/silicon prototyping platform was developed for bulk property measurement via transmission spectroscopy. To obtain phase diagrams of CPH/SA, the applied gradient libraries were annealed using a custom-built temperature gradient stage outfitted with atmospheric control. Optical microscopy was used to locate the miscibility phase boundary marked by differential microstructure induced opacity fluctuations (cloud points). Results were compared with theoretical phase diagrams derived from the application of Flory−Huggins theory of binary polymer miscibility and with AFM experiments on blend libraries and excellent agreement was obtained with the results from the combinatorial methods. The combinatorial methods correctly predict that the poly(SA)/poly(CPH) blend system exhibits UCST behavior. The synergistic effects of combining disposable thiolene/silicon discrete arrays with bulk property measurement by high throughput transmission FTIR have vast application potential in material synthesis and characterization. The results of this study imply the adaptability of generalized combinatorial and high throughput techniques to study the phase behavior of other polymer systems. Indeed, these techniques are amenable to other high throughput studies in biomaterials science including cell viability, cell activation, and protein/biomaterial interactions.

Acknowledgment. The authors acknowledge financial support from the Institute for Combinatorial Discovery at Iowa State University.

References and Notes

(1) Peppas, N. A.; Langer, R. *Science* **1994**, *263* (5154), 1715–20.
(2) Kipper, M. J.; Hou, S.-S.; Seifert, S.; Thiyagarajan, P.; Schmidt-Rohr, K.; Narasimhan, B. *Macromolecules* **2005**, *38*, 8468–8472.
(3) Shen, E.; Pizsczek, R.; Dziadul, B.; Narasimhan, B. *Biomaterials* **2001**, *22* (3), 201–210.
(4) Shen, E.; Kipper, M. J.; Dziadul, B.; Lim, M.-K.; Narasimhan, B. *J. Controlled Release* **2002**, *82* (1), 115–125.
(5) Leong, K. W.; Brott, B. C.; Langer, R. *J. Biol. Mat. Res.* **1985**, *19* (8), 941–55.
(6) Narasimhan, B.; Kipper, M. J. *Adv. Chem. Eng.* **2004**, *29*, 169–218.
(7) Larobina, D.; Kipper, M. J.; Mensitieri, G.; Narasimhan, B. *AIChE J.* **2002**, *48* (12), 2960–2970.
(8) Kipper, M. J.; Narasimhan, B. *Macromolecules* **2005**, *38*, 1989–1999.
(9) Cabral, J. T.; Hudson, S. D.; Harrison, C.; Douglas, J. F. *Langmuir* **2004**, *20* (23), 10020–10029.
(10) Cabral, J. T.; Karim, A. *Measurement Science and Technology* **2005**, *16* (1), 191–198.
(11) Harrison, C.; Cabral, J.; Stafford, C. M.; Karim, A.; Amis, E. J. *Micromechan. Microeng.* **2004**, *14* (1), 153–158.
(12) Meredith, J. C.; Karim, A.; Amis, E. J. *Macromolecules* **2000**, *33* (16), 5760–5762.
(13) Vogel, B.; Cabral, J. T.; Eidelman, N.; Narasimhan, B.; Mallapragada, S. *J. Comb. Chem.* **2005**, *7*921–928.
(14) Kipper, M. J.; Seifert, S.; Thiyagarajan, P.; Narasimhan, B. *Polymer* **2004**, *45* (10), 3329–3340.
(15) Conix, A. J. *Macromol. Syn.* **1966**, *2*, 95–9.
(16) Domb, A. J.; Langer, R. *J. Polym. Sci., Part A: Polym. Chem.* **1987**, *25* (12), 3373–86.
(17) Kipper, M. J.; Shen, E.; Determan, A.; Narasimhan, B. *Biomaterials* **2002**, *23* (22), 4405–4412.
(18) Khoury, C.; Mensing, G. A.; Beebe, D. J. *Lab Chip* **2002**, *2* (1), 50–55.
(19) Gorga, R. E.; Jablonski, E. L.; Thiyagarajan, P.; Seifert, S.; Narasimhan, B. *J. Polym. Sci.* **2002**, *40* (3), 255–271.
(20) Devore, J. L. *Probability and Statistics for Engineering and the Sciences*, 5th ed.; Duxbury: Pacific Grove, 2000; p 1−775.
(21) Sormana, J.-L.; Meredith, J. C. *Macromolecules* **2004**, *37* (6), 2186–2195.
(22) Eidelman, N.; Simon, C. G. *J. Res. Natl. Inst. Standards Technol.* **2004**, *109* (2), 219–231.
(23) Simon, C. G.; Eidelman, N.; Deng, Y.; Washburn, N. R. *Macromol. Rapid Commun.* **2004**, *25* (24), 2003–2007.
(24) Simon, C. G.; Eidelman, N.; Kennedy, S. B.; Sehgal, A.; Khatri, C. A.; Washburn, N. R. *Biomaterials* **2005**, *26* (34), 6909–6915.
(25) Martin, T. P.; Gleason, K. K. *Chem. Vap. Deposition* **2006**, *12* (11), 685–691.
(26) Leugers, A.; Neithamer, D. R.; Sun, L. S.; Hetzner, J. E.; Hilty, S.; Hong, S.; Krause, M.; Beyerlein, K. *J. Comb. Chem.* **2003**, *5* (3), 238–244.
(27) Kipper, M. J.; Seifert, S.; Thiyagarajan, P.; Narasimhan, B. *J. Polym. Sci. Part B−Polym. Phys.* **2005**, *43*, 463–477.

CC900039K